Physics of Plasmas

Hall magnetohydrodynamic effects for current sheet flapping oscillations related to the magnetic double gradient mechanism

Cite as: Phys. Plasmas **17**, 060703 (2010); https://doi.org/10.1063/1.3439687
Submitted: 15 March 2010 . Accepted: 10 May 2010 . Published Online: 16 June 2010

N. V. Erkaev, V. S. Semenov, and H. K. Biernat


View Online


Export Citation

ARTICLES YOU MAY BE INTERESTED IN

The mechanisms of electron heating and acceleration during magnetic reconnection
Physics of Plasmas **21**, 092304 (2014); https://doi.org/10.1063/1.4894484

Current sheet oscillations in the magnetic filament approach
Physics of Plasmas **19**, 062905 (2012); https://doi.org/10.1063/1.4725506

The process of electron acceleration during collisionless magnetic reconnection
Physics of Plasmas **13**, 012309 (2006); https://doi.org/10.1063/1.2164808

AIP Publishing

© 2010 American Institute of Physics.

Hall magnetohydrodynamic effects for current sheet flapping oscillations related to the magnetic double gradient mechanism

N. V. Erkaev,[1] V. S. Semenov,[2] and H. K. Biernat[3]
[1]*Institute of Computational Modelling, SB RAS, and Siberian Federal University, Krasnoyarsk, Russia*
[2]*Institute of Physics, State University of St. Petersburg, St. Petersburg, Russia*
[3]*Space Research Institute, Austrian Academy of Sciences, Graz A-8042, Austria and Institute of Physics, University of Graz, Graz, Austria*

(Received 15 March 2010; accepted 10 May 2010; published online 16 June 2010)

Hall magnetohydrodynamic model is investigated for current sheet flapping oscillations, which implies a gradient of the normal magnetic field component. For the initial undisturbed current sheet structure, the normal magnetic field component is assumed to have a weak linear variation. The profile of the electric current velocity is described by hyperbolic functions with a maximum at the center of the current sheet. In the framework of this model, eigenfrequencies are calculated as functions of the wave number for the "kink" and "sausage" flapping wave modes. Because of the Hall effects, the flapping eigenfrequency is larger for the waves propagating along the electric current, and it is smaller for the opposite wave propagation with respect to the current. The asymmetry of the flapping wave propagation, caused by Hall effects, is pronounced stronger for thinner current sheets. This is due to the Doppler effect related to the electric current velocity.
© *2010 American Institute of Physics*. [doi:10.1063/1.3439687]

The term "flapping" waves was introduced with regard to the up-down motions of the current sheet in the Earth's magnetotail. These flapping wave oscillations were indicated usually by measurements of the corresponding variations in the tangential magnetic field component from negative to positive values. In fact, there exist many observations[1–6] demonstrating existence of the "kinklike" disturbances of the magnetotail current sheet, which propagate along the plane of the sheet perpendicular to the ambient magnetic field. Statistical studies[7,8] proved a relationship between the flapping oscillations and fast plasma flows in the current sheet. In spite of a large amount of existing observations, a physical nature of the flapping motions is still not understood well. There exist several theoretical approaches for describing the flapping waves in the Earth's current sheet. In particular, a drift kink mode[9] was proposed to explain the flapping oscillations, which are due to a relative drift of electrons and protons. The ion/ion drift kink mode was also considered,[10] which has a larger growth rate compared to the electron/proton drift model. Recently the drift eigenmodes for a one-dimensional kinetic current sheet were investigated,[11] taking into account the anisotropy of ion distributions and quasiadiabatic ion motions. In the framework of the magnetohydrodynamic (MHD) approach, two models were elaborated. One of them is the ballooning-type mode in the curved current sheet magnetic field.[12] For this case, the magnetic curvature radius is required to be larger than the flapping wavelength. Another MHD model[13] claimed that the MHD flapping modes can appear due to the gradient of the normal magnetic field component along the current sheet. This model, called the "magnetic double gradient mechanism," yields the characteristic flapping frequency determined by a product of two magnetic gradients. Recently it was used for comparison with Cluster data.[14] The results of the comparison indicate that the model[13] gives quite good fit to the observations. In the present paper we extend the theoretical model based on the "magnetic double gradient mechanism"[13] taking into account Hall MHD effects. These effects are expected to be rather important for thin current sheets, especially in cases when the electric current is carried mainly by protons, and the current velocity is of the same order as the flapping wave phase velocity.

A geometrical situation of the problem and the Cartesian coordinate system are illustrated in Fig. 1, which shows a wavy neutral sheet. The undisturbed current sheet is assumed to be parallel to the xy plane. The z axis is perpendicular to the current sheet, and the undisturbed electric current J is directed along the y axis, as shown is the figure. We apply a system of Hall MHD for nonstationary variations in plasma sheet parameters

$$nm_p\left(\frac{\partial \mathbf{V}}{\partial t}+\mathbf{V}\cdot\nabla\mathbf{V}\right)+\nabla P=\frac{1}{\mu_0}\mathbf{B}\cdot\nabla\mathbf{B}, \tag{1}$$

$$\frac{\partial \mathbf{B}}{\partial t}-\nabla\times(\mathbf{V}_e\times\mathbf{B})=0, \tag{2}$$

$$\mathbf{V}_e=\mathbf{V}-\mathbf{U},\quad \mathbf{U}=\frac{1}{\mu_0 ne}\nabla\times\mathbf{B}, \tag{3}$$

$$\frac{\partial n}{\partial t}+\mathbf{V}\cdot\nabla n=0,\quad \nabla\cdot\mathbf{V}=0,\quad \nabla\cdot\mathbf{B}=0. \tag{4}$$

Here $\mathbf{V}$ and $\mathbf{V}_e$ are the velocities of the protons and electrons, $\mathbf{U}$ is the electric current velocity, $\mathbf{B}$ is the magnetic field vector, and m_p, n, and P are the proton mass, plasma density, and total pressure, respectively. The total pressure is defined as the sum of the magnetic and plasma pressures. We consider specific wave perturbations propagating across the magnetic field lines, which are much slower than the mag-

 © 2010 American Institute of Physics

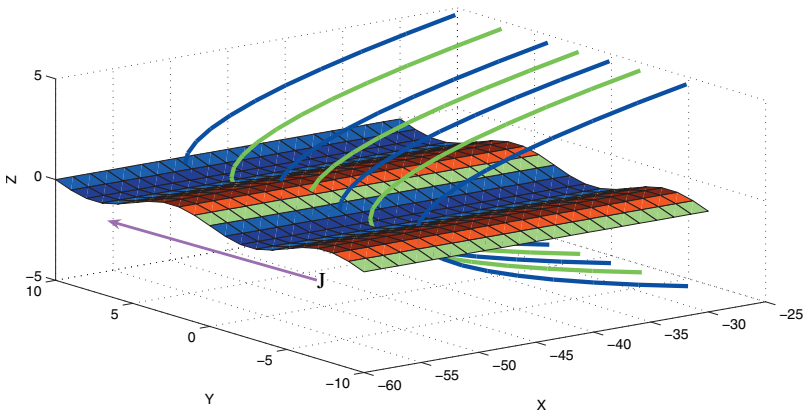

FIG. 1. (Color) Geometrical situation of the problem.

netosonic modes. In this case the incompressible approximation ($\nabla\cdot\mathbf{V}=0$) can be applied. In this approach,[13] we focus our study on the very slow wave modes existing only in the presence of the gradient of the B_z component in the magnetotail current sheet along the x direction. We consider a current sheet with a nonzero normal magnetic field component (B_z), which has weak variation along the x coordinate. The undisturbed electric current velocity is considered to be equal to the proton velocity, and thus $\mathbf{V}_e=0$. With this assumption, the undisturbed magnetic field, bulk, and current velocities are given as follows:

$$\mathbf{B}=[B_x(z),0,B_z(x)],\quad \mathbf{V}=(0,V_0,0),$$
$$V_0=\frac{1}{\mu_0 ne}\frac{\partial B_x}{\partial z}. \tag{5}$$

Considering the electric current to be carried only by protons, we expect to get the most strongly pronounced Hall MHD effects.

We introduce small perturbations of the magnetic field, velocity, and total pressure,

$$\mathbf{B}=[(B_x+b_x),b_y,(B_z+b_z)],\quad \mathbf{V}_e=(v_{ex},v_{ey},v_{ez}),$$
$$P=P_0+p,\quad \mathbf{V}=(v_x,V_0+v_y,v_z). \tag{6}$$

We assume the magnetic gradient $\partial B_z/\partial x$ to be constant and consider all wave perturbations to be functions of time and two Cartesian coordinates (y,z). Therefore we cancel the derivatives of the perturbations with respect to the x coordinate. Using these assumptions and linearizing the initial system of equations, we obtain

$$nm_p\left(\frac{\partial v_x}{\partial t}+V_0\frac{\partial v_x}{\partial y}\right)+\nabla_x p=\frac{1}{\mu_0}\left(b_z\frac{\partial B_x}{\partial z}+B_z\frac{\partial b_x}{\partial z}\right), \tag{7}$$

$$nm_p\left(\frac{\partial v_y}{\partial t}+V_0\frac{\partial v_y}{\partial y}\right)+\nabla_y p=\underline{\frac{1}{\mu_0}B_z\frac{\partial b_y}{\partial z}}, \tag{8}$$

$$nm_p\left(\frac{\partial v_z}{\partial t}+V_0\frac{\partial v_z}{\partial y}\right)+\nabla_z p=\frac{1}{\mu_0}\left(b_x\frac{\partial B_z}{\partial x}+\underline{B_z\frac{\partial b_z}{\partial z}}\right), \tag{9}$$

$$\frac{\partial b_x}{\partial t}+V_0\frac{\partial b_x}{\partial y}+v_z\frac{\partial B_x}{\partial z}-B_z\frac{\partial v_x}{\partial z}=0, \tag{10}$$

$$\frac{\partial b_y}{\partial t}-B_z\frac{\partial v_y}{\partial z}+B_z\frac{\partial}{\partial z}\left(\frac{1}{\mu_0 ne}\frac{\partial b_x}{\partial z}\right)=0, \tag{11}$$

$$\frac{\partial b_z}{\partial t}+v_x\frac{\partial B_z}{\partial x}-\underline{\frac{1}{\mu_0 ne}\frac{\partial b_z}{\partial y}\frac{\partial B_z}{\partial x}}-B_z\frac{\partial v_z}{\partial z}-B_z\frac{\partial}{\partial z}\left(\frac{1}{\mu_0 ne}\frac{\partial b_x}{\partial y}\right)=0, \tag{12}$$

$$\frac{\partial v_z}{\partial z}+\frac{\partial v_y}{\partial y}=0. \tag{13}$$

We also neglect the underlined terms in the equations above, which are on the order of B_z^2. Inserting Fourier harmonics $\propto\exp(-i\omega t+iky)$ into the linearized equations, we obtain

$$-inm_p\Omega v_x=\frac{1}{\mu_0}\left(b_z\frac{\partial B_x}{\partial z}+B_z\frac{\partial b_x}{\partial z}\right), \tag{14}$$

$$-nm_p\Omega v_y+kp=0, \tag{15}$$

$$-inm_p\Omega v_z+\frac{\partial p}{\partial z}=\frac{1}{\mu_0}\left(b_x\frac{\partial B_z}{\partial x}\right), \tag{16}$$

$$-i\Omega b_x+v_z\frac{\partial B_x}{\partial z}-B_z\frac{\partial v_x}{\partial z}=0, \tag{17}$$

$$-i\omega b_y-B_z\frac{\partial v_y}{\partial z}+B_z\frac{\partial}{\partial z}\left(\frac{1}{\mu_0 ne}\frac{\partial b_x}{\partial z}\right)=0, \tag{18}$$

$$-i\omega b_z+v_x\frac{\partial B_z}{\partial x}-B_z\frac{\partial v_z}{\partial z}-B_z\frac{\partial}{\partial z}\left(\frac{ikb_y}{\mu_0 ne}\right)=0,$$
$$\frac{\partial v_z}{\partial z}+ikv_y=0, \tag{19}$$

where $\Omega=\omega-kV_0$. Finally, the system of equations (14)–(19) can be reduced to the second order ordinary equation for the velocity perturbation v_z,

$$\frac{1}{\rho\Omega}\frac{\partial}{\partial z}\left(\rho\Omega\frac{\partial v_z}{\partial z}\right)-k^2v_z\left(1-\frac{1}{\mu_0\rho\Omega^2}\frac{\partial B_x}{\partial z}\frac{\partial B_z}{\partial x}\right)=0. \tag{20}$$

The frequency ω can be determined by solving Eq. (20) with the usual boundary conditions for the perturbations, which

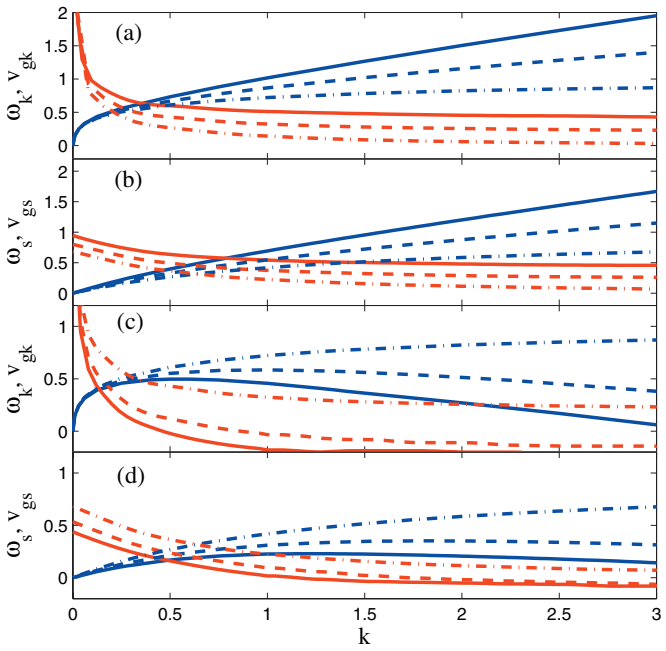

FIG. 2. (Color) Flapping frequencies and group velocities for the kink and "sausage" modes ($\lambda=0.2$); plots (a) and (b) are for the wave propagation along the electric current; plots (c) and (d) are for the opposite propagation (against electric current). The solid, dashed, and dot-dashed curves correspond to $\alpha=0.4, 0.2, 0$, respectively.

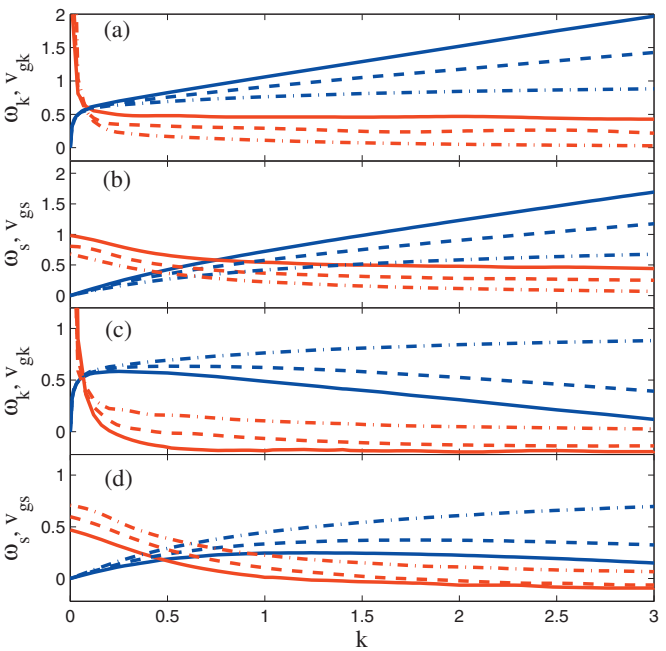

FIG. 3. (Color) Similar to Fig. 2, but for $\lambda=0.4$.

are set to vanish at infinity. We introduce dimensionless quantities marked by tilde, which are very convenient for solving the boundary value problem

$$\tilde{n}=n/n_0, \quad \tilde{z}=z/\Delta, \quad \tilde{\omega}=\omega/\omega_f, \quad \tilde{k}=k\Delta,$$

$$\tilde{V}_0=V_0/V_{0\,\max}, \quad V_{0\,\max}=\frac{1}{\mu_0 n_0 e}\left.\frac{\partial B_x}{\partial z}\right|_{z=0}, \tag{21}$$

$$\omega_f=\left.\left(\frac{1}{\mu_0 m_p n_0}\frac{\partial B_x}{\partial z}\frac{\partial B_z}{\partial x}\right)^{1/2}\right|_{z=0},$$

where Δ is a half thickness of the current sheet and n_0 is the plasma density at the center of the current sheet. With this normalization, Eq. (20) reads

$$\frac{1}{\tilde{n}\tilde{\Omega}}\frac{\partial}{\partial z}\left(\tilde{n}\tilde{\Omega}\frac{\partial v_z}{\partial z}\right)-\tilde{k}^2 v_z\left(1-\frac{\tilde{V}_0}{\tilde{\Omega}^2}\right)=0. \tag{22}$$

Here $\tilde{\Omega}=\tilde{\omega}-\alpha k\tilde{V}_0$, α is the dimensionless parameter characterizing Hall effects, and $\alpha=V_{0\,\max}/\omega_f\Delta$. We assume model analytical formulas for the magnetic field and plasma density variations across the current sheet

$$\tilde{B}_x=\tanh(z/\Delta), \quad \tilde{n}=\frac{1}{\cosh^2(\lambda z/\Delta)}, \tag{23}$$

where λ is a free parameter which determines a shape of the current velocity profile. In particular, for $\lambda=1$ we have a constant current velocity that is relevant to the Harris-like current sheet. Taking this parameter in a range $0<\lambda<1$, we get the current velocity profile with a maximum at the center of the current sheet. Therefore, this parameter characterizes a deviation of the current velocity profile from that of Harris.

The eigenvalue problem was solved numerically using a standard method. Figure 2 shows the calculated flapping frequencies (blue curves) and group velocities (red curves) for the current velocity profile corresponding to $\lambda=0.2$. From top to bottom, shown are the dispersion curves and group velocities for the kink (ω_k, V_{gk}) and sausage (ω_s, V_{gs}) flapping wave modes propagating along the electric current [(a) and (b)], and also in the opposite direction [(c) and (d)]. In each plot, the solid, dashed, and dot-dashed curves correspond to the different values of the Hall parameter: $\alpha=0.4$ (solid), $\alpha=0.2$ (dashed), and $\alpha=0$ (dot-dashed), respectively. Figure 3 is similar to Fig. 2, but for another current velocity profile characterized by $\lambda=0.4$. The figures demonstrate the influence of the Hall parameter on the flapping wave eigenfrequency and group velocity in dependence on the direction of wave propagation with respect to the electric current.

In the particular case of the flapping wave propagation in the direction of the electric current, the eigenfrequency has monotonic behavior as a function of the wave number. An increase in the Hall parameter leads to an enhancement in the eigenfrequency, which has a linear asymptotic behavior for large wave numbers. In the opposite case, when the wave vector is antiparallel to the current velocity, the eigenfrequency is a nonmonotonic function of the wave number: it increases first to a maximal value, and then decreases to zero. As one can see from the figures, the maximal eigenfrequency is smaller for larger values of the Hall parameter, which suppresses the flapping waves propagating against the electric current. For example, we estimate the flapping frequency for the magnetic field and plasma parameters, which are reasonable for the current sheet conditions in the Earth's magnetotail,

$$B_x = 20 \text{ nT}, \quad B_z = 2 \text{ nT}, \quad \Delta \sim R_E, \quad n_p = 0.3 \text{ cm}^{-3},$$
$$k\Delta = 1, \quad \partial B_z/\partial x \sim B_z/L_x, \quad L_x \sim 4R_E, \tag{24}$$

where R_E is the radius of Earth. For these parameters we estimate the electric current velocity $V_{0\,\max}$, frequency ω_f, and the Hall parameter α,

$$V_{0\,\max} \approx 52 \text{ km/s}, \quad \omega_f \Delta \approx 126 \text{ km/s},$$
$$\alpha \approx 0.4, \quad \omega_f \approx 0.02c^{-1}. \tag{25}$$

Using Fig. 2(a), we find eigenfrequency, group velocity, and periods for the flapping waves, when the wave vector has the same direction as the electric current. In particular, for $\alpha=0.4$ (solid curve) and $k\Delta=1$ we estimate

$$\omega_+ \approx 0.02 \text{ s}^{-1}, \quad T \approx 5 \text{ min}, \quad V_{gk} \approx 63 \text{ km/s}. \tag{26}$$

Using Fig. 2(c), solid curve, we estimate the eigenfrequencies and periods for the flapping waves propagating in the opposite direction with respect to the electric current vector. The group velocity is positive for sufficiently small wave numbers $k\Delta \leq 0.5$. This means that only long waves can propagate against electric current. In particular, for $k\Delta=0.25$ we find

$$\omega_- \approx 0.009 \text{ s}^{-1}, \quad T \approx 12 \text{ min}, \quad V_{gk} \approx 25 \text{ km/s}. \tag{27}$$

This example illustrates that the flapping waves, propagating in the direction of the electric current, have substantially larger frequency and group speed, compared to those propagating to the opposite direction. The described above Hall effects explain the large variability of the flapping frequencies observed by satellites Cluster and Themis.

First statistical studies of the Cluster mission[2] yield a conclusion that flapping waves propagate preferably from the tail center to its periphery. This result was also consistent with previous observations. However the dawn-dusk asymmetry aspects were not discussed. Further analysis of Cluster data[7] indicated some evidence of the flapping propagation asymmetry: the durations of current sheet crossings were plotted versus distances across the tail (Ygsm), and the flapping periods were shown to be somewhat smaller for the positive Ygsm coordinates (duskward side) compared to those for the negative Ygsm (dawnward side).

It is worth noting that the favored propagation of the flapping waves in the direction of the current found in our study is the reverse to that of the waves discovered in three-dimensional simulation of magnetic reconnection.[15] But the latter seems to be related to another conditions in the vicinity of the X line, where the electric current was carried only by electrons. Our asymmetry effect for flapping waves is related to the proton current speed, which is assumed to be dominant in our model.

In summary, we have analyzed flapping wave oscillations in the magnetotail current sheet taking into account a gradient of the normal magnetic field component, and also Hall MHD effects. We assumed that the initial undisturbed electric current is carried mainly by protons. With this assumption, the Hall MHD effects are pronounced stronger compared to cases when the electric current is provided partially by electrons. The role of Hall effects is determined by the dimensionless Hall parameter α which is a ratio of the maximal proton current speed to the characteristic flapping speed. The latter is proportional to the square root of the product of two magnetic gradients. The flapping eigenfrequencies are calculated for "kink" and "sausage" modes. The Hall effects look similar for both modes. For the same wavelength, the flapping eigenfrequency is much larger for the parallel wave propagation then that for the antiparallel propagation, with respect to the electric current. Therefore, the Hall effects may cause a strong asymmetry of the flapping wave propagations from the center to the flanks of the current sheet. They are in favor to the flapping waves propagating in the electric current direction, and they suppress the waves propagating in the opposite direction. A physical reason for this asymmetry is the Doppler effect which is caused by the proton current velocity. The range of the observed flapping frequency variations can be interpreted due to the Hall effects, depending on the current sheet properties, and direction of the flapping wave propagation.

This work is supported by RFBR (Grant Nos. N 07-05-00776-a and N 09-05-91000-ANF_a), and by Program No. 16 of RAS. Additional support is due to the Austrian "Fonds zur Förderung der wissenschaftlichen Forschung" under Project No. I 193-N16 and the "Verwaltungsstelle für Auslandsbeziehungen" of the Austrian Academy of Sciences.

[1] T. L. Zhang, W. Baumjohann, R. Nakamura *et al.*, Geophys. Res. Lett. **29**, 1899, doi:10.1029/2002GL015544 (2002).
[2] V. A. Sergeev, A. Runov, W. Baumjohann, R. Nakamura, T. L. Zhang, A. Balogh, P. Louard, J.-A. Sauvaud, and H. Reme, Geophys. Res. Lett. **31**, L05807, doi:10.1029/2003GL019346 (2004).
[3] A. Runov, V. A. Sergeev, W. Baumjohann *et al.*, Ann. Geophys. **23**, 1391 (2005).
[4] A. V. Runov, A. Sergeev, R. Nakamura *et al.*, Ann. Geophys. **24**, 247 (2006).
[5] A. A. Petrukovich, T. L. Zhang *et al.*, Ann. Geophys. **24**, 1695 (2006).
[6] C. Shen, Z. J. Rong, X. Li *et al.*, Ann. Geophys. **26**, 3525 (2008).
[7] V. A. Sergeev, D. A. Sormakov, S. V. Apatenkov *et al.*, Ann. Geophys. **24**, 2015 (2006).
[8] C. Gabrielse, V. Angelopoulos, A. Runov, L. Kepko, K. H. Glassmeier, H. U. Auster, J. McFadden, C. W. Carlson, and D. Larson, Geophys. Res. Lett. **35**, L17S13, doi:10.1029/2008GL033664 (2008).
[9] W. Daughton, J. Geophys. Res. **104**, 701 (1990).
[10] H. Karimabadi, P. L. Pritchett, W. Daughton, and D. Krauss-Varban, J. Geophys. Res. **108**, 1401, doi:10.1029/2003JA010109 (2003).
[11] L. M. Zeleni, A. V. Artem'ev, A. A. Petrukovich *et al.*, Ann. Geophys. **27**, 861 (2009).
[12] I. V. Golovchanskaya and Y. P. Maltsev, Geophys. Res. Lett. **32**, L02102, doi:10.1029/2004GL021552 (2005).
[13] N. V. Erkaev, V. S. Semenov, I. V. Kubyshkin, M. V. Kubyshkina, and H. K. Biernat, J. Geophys. Res. **114**, A03206, doi:10.1029/2008JA013728 (2009).
[14] C. Forsyth, M. Lester, R. C. Fear *et al.* Ann. Geophys. **27**, 2457 (2009).
[15] J. D. Huba and L. I. Rudakov, Phys. Plasmas **9**, 4435 (2002).